Endothelin Receptor Dimers Evaluated by FRET, Ligand Binding, and Calcium Mobilization

Nathan J. Evans and Jeffery W. Walker
Department of Physiology, University of Wisconsin, Madison, Wisconsin

ABSTRACT Endothelin-1 (ET-1) mediates physiological responses via endothelin A (ET_A) and B (ET_B) receptors, which may form homo- and heterodimers with unknown function. Here, we investigated ET-receptor dimerization using fluorescence resonance energy transfer (FRET) between receptors tagged with CFP (donor) and receptors tagged with tetracysteine-FlAsH (fluorescein arsenical hairpin) (acceptor) expressed in HEK293 cells. FRET efficiencies were 15%, 22%, and 27% for ET_A/ET_A, ET_B/ET_B, and ET_A/ET_B, respectively, and dimerization was further supported by coimmunoprecipitation. For all dimer pairs, the natural but nonselective ligand ET-1 rapidly (≤30 s) reduced FRET by >50%, but did not detectably reduce coimmunoprecipitation. ET-1 stimulated a transient increase in intracellular Ca^{2+} ($[Ca^{2+}]_i$) lasting 1–2 min for both homodimer pairs, and these ET-1 actions on FRET and $[Ca^{2+}]_i$ elevation were blocked by the appropriate subtype-selective antagonist. In contrast, ET_A/ET_B heterodimers mediated a sustained $[Ca^{2+}]_i$ increase lasting >10 min, and required a combination of ET_A and ET_B antagonists to block the observed FRET and $[Ca^{2+}]_i$ responses. The sensitive CFP/FlAsH FRET assay used here provides new insights into endothelin-receptor dimer function, and represents a unique approach to characterize G-protein-coupled receptor oligomers, including their pharmacology.

INTRODUCTION

Endothelins (ETs) are composed of a family of 21 amino acid peptides (ET-1, ET-2, and ET-3) that regulate many physiological systems (1). ET-1 is the predominant endothelin in the cardiovascular system, where it binds to two distinct class A G-protein-coupled receptor (GPCR) subtypes, endothelins A (ET_A) and B (ET_B) (2,3). Despite 59% amino acid sequence identity, the ET_A and ET_B receptors function and internalize with distinct patterns. Whereas ET_A stimulation leads to increased cardiac inotropy and vasoconstriction, ET_B stimulation results in vasodilation and possibly ET-1 clearance (4–7). Although both receptors are internalized in a similar fashion that depends upon G-protein-coupled receptor kinase, arrestin, clathrin-coated pits, and dynamin, they appear to be targeted to different intracellular fates. Once internalized, the ET_A receptor recycles back to the plasma membrane, whereas the ET_B receptor is targeted to lysosomes for degradation (8–10). The targeting of ET_B receptors for lysosomal degradation could explain the ET-1 clearance role proposed for this receptor.

Emerging evidence suggests that GPCRs are capable of forming both homo- and heterodimers that influence receptor trafficking and function (11–13). Maturation of $GABA_B$ receptors requires receptor dimerization at the Golgi to be N-glycosylated for membrane trafficking (14). Altered receptor pharmacology and function were seen in β1 and β2 adrenergic receptors in intact adult mouse cardiomyocytes, where heterodimerization reduced spontaneous receptor activity and enhanced responsiveness to catecholamines (15). In addition, evidence for GPCR dimers has been obtained in vivo. In a study examining angiotensin and β-adrenergic receptor heterodimers in mice, an AT-1 receptor blocker decreased catecholamine-induced elevations in heart rate by uncoupling β-adrenergic receptors from G_s (16). Finally, models based on the crystal structure of bovine rhodopsin suggest that dimers may be required to provide an optimal footprint for G-protein insertion (17).

Despite coexpression of ET-receptor subtypes in a variety of cells, little is known about their dimerization capabilities. In astrocytes, where both ET_A and ET_B receptors may control ET-1 clearance, addition of both ET_A and ET_B selective antagonists (but not their individual application) was required to block ET-1 uptake (18). It has also been suggested that ET-1 can function as a bivalent ligand that binds to the ET_A receptor via its N-terminus and to the ET_B receptor via its C-terminus, thereby inducing ET heterodimer formation through a ligand bridge (19). The most direct evidence for ET_A and ET_B homo- and heterodimers has emerged from studies that combined extensive analysis of coimmunoprecipitation of tagged receptors with measurements of fluorescence resonance energy transfer (FRET) using the cyan/yellow fluorescent protein (CFP/YFP) FRET pair (20,21). These initial investigations indicated considerable complexity of ET-receptor interactions and suggested the need for further experimentation to elucidate the dynamics and functional consequences of their interactions.

In this study, using a different FRET pair, we examined the ability of ET_A and ET_B receptors to form dimers and endeavored to put the results into a physiological context by measuring receptor function in parallel. CFP-tagged ET receptors were used as the FRET donor, whereas the commercially

Submitted August 8, 2007, and accepted for publication March 7, 2008.

Address reprint requests to Jeffery W. Walker, Dept. of Physiology, 1300 University Ave., Madison, WI 53706. Tel.: 608-262-6941; Fax: 608-265-5512; E-mail: jwalker@physiology.wisc.edu.

Editor: David W. Piston.

0006-3495/08/07/483/10 $2.00

doi: 10.1529/biophysj.107.119206

available reagent FlAsH (fluorescein arsenical hairpin) was used in place of the traditional acceptor YFP to exploit two experimental advantages. The green spectral shift of FlAsH provided greater spectral overlap with CFP, allowing for enhanced energy transfer between donor and acceptor (22). Use of the FlAsH binding motif of 17 amino acids eliminated the need for a second large 238-amino-acid fluorescent protein probe (i.e., YFP) that could influence receptor function or orientation in the membrane (22–26). Since FRET interactions between a donor and acceptor are rapid and limited to distances of <10 nm, we sought evidence for ''short-range'' protein-protein interactions that were dynamic and functionally relevant. Functional consequences of ET receptor dimerization were investigated by monitoring intracellular calcium changes using Ca^{2+}-sensitive fluorescent dyes. We conclude from this study that the CFP/FlAsH FRET pair has significant advantages over CFP/YFP for monitoring conformational changes in ET receptor dimers. Moreover, the results provide evidence that ET receptor heterodimers have pharmacological and Ca^{2+} signaling properties distinct from other forms of these receptors.

MATERIALS AND METHODS

Materials

Reagents were obtained from Sigma Chemical Company (St. Louis, MO), unless otherwise stated. TransIT-LT1 was from Mirus (Madison, WI); HEK293 cells from Stratagene (La Jolla, CA); X-rhod-1-AM, Fluo-4-AM, TC-FlAsH II, Hank's balanced salt solution (HBSS), Opti-MEM, horse serum, and G418 from Invitrogen (Carlsbad, CA); cell culture plates from BD Biosciences (Franklin Lakes, NJ); monoclonal CFP antibody (JL-8) and pECFP-N1 plasmid vector from Clontech (Mountain View, CA); monoclonal c-myc (9E10) from Covance (Berkeley, CA); and protein G-sepharose 4 fast flow from GE Healthcare (Piscataway, NJ).

Generation of receptor constructs

Full-length human ET_A (1–427) and ET_B (1–442) receptor cDNA was obtained from the University of Missouri-Rolla (http://www.cdna.org). ET_A cDNA (GenBank accession number AY275462) was inserted in frame into the pECFP-N1 plasmid vector at NheI-AgeI sites to create a fused protein construct (ET_A-CFP). The c-myc epitope tag was inserted in frame onto the N-terminus of ET_A at NheI-*Hin*dIII sites, and a 17-amino-acid tetracysteine binding sequence (AEAAAREA**CCPGCC**ARA) was inserted onto the C-terminus of ET_A at SalI-NotI sites in frame (myc-ET_A-C4). ET_B cDNA (GenBank AY275463) was inserted in frame into the pECFP-N1 vector at NheI-AgeI sites to create a fused protein construct (ET_B-CFP). The c-myc epitope tag was inserted in frame onto the N-terminus of ET_B at NheI-*Hin*dIII sites and the tetracysteine binding sequence onto the C-terminus of ET_B at SalI-NotI sites in frame (myc-ET_B-C4).

Cell culture

HEK293 cells were maintained in minimal essential medium (MEM-α) supplemented with 10% horse serum and antibiotics (50 units/mL penicillin, 50 μg/mL streptomycin, Gibco, Carlsbad, CA). Cells were grown at 37°C with 95% air, 5% CO_2, and 25% humidity.

HEK293 cell transfection

Stable cell lines of myc-ET_A-C4 and myc-ET_B-C4 were created using LT-1 transfection reagent according to manufacturer instructions. Selection and maintenance was obtained using MEM-α supplemented with 10% horse serum and G418. Transient transfection of ET_A-CFP and ET_B-CFP constructs into stable cell lines was performed using LT-1.

Immunoprecipitation/immunoblotting

HEK293 cells stably expressing myc-ET_A-C4 or myc-ET_B-C4 on 10-cm plates were transiently transfected with ET_A-CFP or ET_B-CFP and incubated in growth media for 48 h. Cells were washed with phosphate-buffered saline and permeabilized in lysis buffer (in mM, 150 NaCl, 25 Tris-HCl, 1 EDTA, 1 EGTA, 1 sodium orthovanadate, 1 sodium fluoride, and protease inhibitor cocktail tablet, pH 7.4) with 1% Triton X-100 for 5 min on ice. In case of drug treatment, cells were incubated with ET-1 or sarafotoxin s6c for 10 min at room temperature before washing and cell lysis. Cells were scraped off with a cell lifter, incubated in lysis buffer for 30 min on ice, and then spun at $13{,}000 \times g$ for 10 min at 4°C. The supernatant was incubated in 5 mg of monoclonal anti-c-myc antibody overnight at 4°C with gentle rocking, followed by a 3-h incubation in protein G sepharose beads. Beads were then thoroughly washed in lysis buffer and eluted with sodium dodecyl sulfate (SDS) sample buffer. Samples were run on 12% SDS-polyacrylamide gels and transferred to polyvinylidene fluoride membranes. Immunoblot analyses were conducted with monoclonal anti-CFP primary antibody and horseradish peroxidase-conjugated secondary antibody from Santa Cruz Biotechnologies (Santa Cruz, CA).

Ca^{2+} indicator measurements

HEK293 cells stably expressing myc-ET_A-C4 or myc-ET_B-C4 on glass-bottom culture dishes from MatTek (Ashland, MA) were transiently transfected with ET_A-CFP or ET_B-CFP and incubated for 24 h. Cells were then loaded with 4 μM Fluo-4 or X-rhod-1 in Opti-MEM (Gibco) for 1 h at 37°C. Cells were gently washed and maintained in room-temperature Ringer's solution with or without Ca^{2+} (in mM, 125 NaCl, 5 KCl, 10 HEPES, 5 $MgCl_2$, and 2 Ca^{2+}). Imaging was performed with a Bio-Rad Radiance 2100 MP Rainbow laser scanning confocal microscope equipped with argon gas, mixed gas (helium/neon) and red diode lasers. Changes in Ca^{2+} indicator fluorescence were measured in linescan mode using LaserSharp 6.0 software. Fluo-4 and X-rhod-1 are nonratiometric calcium dyes and were therefore used without calibration (i.e., fluorescence was not converted to free $[Ca^{2+}]_i$).

FRET

HEK293 cells stably expressing myc-ET_A-C4 or myc-ET_B-C4 were grown onto 35-mm culture plates and transiently transfected with ET_A-CFP or ET_B-CFP. Cells were then incubated for 24 h before FlAsH loading. Measurements were made from several individual cells in each culture plate. Normalized fluorescence values for a minimum of four cells from four plates were averaged to obtain data as in Fig. 1 *B*.

FlAsH loading

Culture plates were thoroughly rinsed with commercial HBSS (in g/L, 0.14 $CaCl_2$, 0.4 KCl, 0.06 KH_2PO_4, 0.1 $MgCl_2$, 0.1 $MgSO_4$, 8.0 NaCl, 0.35 $NaHCO_3$, 0.048 Na_2HPO_4, and 1.0 D-glucose) and covered with 500 μL of freshly made loading solution consisting of 10 μM EDT and 1 μM FlAsH-EDT_2 in HBSS. Dishes were incubated at room temperature for 2 h in the dark with gentle shaking. The FlAsH-EDT_2 loading solution was then thoroughly rinsed with HBSS before imaging.

FlAsH unloading

A freshly made stock solution of 15 mM 2,3-dimercapto-1-propanol (BAL) in HBSS was used. The stock solution was diluted threefold in the solution bathing the imaged cells to yield a final BAL concentration of 5 mM. Plates were incubated in the BAL solution for 10 min, followed by image capture.

Microscope

Global epifluorescence was captured with a cooled CCD DP-70 camera (Olympus, Melville, NY) using a 20×/0.95-NA water-immersion objective in an upright Olympus BX51 microscope. Excitation was provided by a 100-W Hg lamp filtered with standard bandpass excitation/emission filter cubes. Chroma 31036 (excitation 436/20 nm, emission 480/30 nm, dichroic 455) was used for CFP, and Chroma 41028 (excitation 500/20 nm, emission 535/30 nm, dichroic 515) was used for FlAsH.

Image analysis

Images of 680 × 512 pixels were acquired at 8-bit resolution without compression of the A/D conversion scale. Integration time (250 ms) and camera sensitivity settings were set constant. Five images were averaged to improve the signal/noise ratio and composite images were analyzed with NIH image software. Mean pixel intensities were measured in regions of interest of 100–200 pixels (0.04 μm/pixel). Background intensities were measured near the regions of interest and were subtracted. Mean pixel intensities for CFP and FlAsH emissions were in the range 30–150 on a scale of 0–255.

FRET ratio/efficiency

FRET is characterized by the increase in acceptor (FlAsH) emission concomitant with a decrease in donor (CFP) emission. This ratio is calculated as follows: (CFP emission after FlAsH loading and after BAL wash)/(CFP emission after FlAsH loading and before BAL wash). From this ratio, the FRET efficiency was determined according to 1 − [1/FRET ratio].

[^{125}I]-ET-1 binding experiments

HEK293 cells stably expressing myc-ET_A-C4 or myc-ET_B-C4 on 35-mm plates were transiently transfected with ET_A-CFP or ET_B-CFP, or mock-transfected, and sustained in growth medium for 24 h. Cells were incubated in 100 pmol [^{125}I]-ET-1 with (nonspecific binding) or without (total binding) pretreatment with 10 nM cold ET-1. Cells were then thoroughly washed with ice-cold phosphate-buffered saline and solubilized with lysis buffer. Samples were spun at 5000 × *g* for 5 min and supernatant was added to 10 mL vials with Bio-Safe II scintillation cocktail (Mount Prospect, IL). Radioactivity was measured in a gamma-counter (PerkinElmer, Boston, MA). Specific binding was taken as the difference between total and nonspecific binding and normalized to milligrams of protein.

Statistics

Paired samples with and without agonist or antagonist were compared with an unpaired two-tailed Student's *t*-test using the commercial software Excel. For statistical analysis of more than two experimental conditions, a one-way ANOVA with Tukey's post-test was applied using a public domain website (http://faculty.vassar.edu/lowry/VassarStats.html). In all cases, values of $p < 0.05$ were taken to represent statistically significant differences.

RESULTS

Expression of endothelin receptor constructs in HEK293 cells

Full-length human endothelin A (ET_A) or B (ET_B) receptors were C-terminally tagged with CFP (ET_A-CFP and ET_B-CFP) or N-terminally tagged with the c-myc epitope and C-terminally tagged with a tetracysteine (C4) motif (myc-ET_A-C4 and myc-ET_B-C4) to create fused receptor constructs. Transient transfection of CFP constructs revealed that typically 30–50% of HEK293 cells expressed the receptor constructs. The myc-ET_A-C4 and myc-ET_B-C4 constructs were each expressed in a separate stable HEK293 cell line to ensure reproducible expression levels in the entire cell population from experiment to experiment. To assure that the CFP and myc/C4-tagged endothelin receptor constructs were properly trafficked to the plasma membrane, transfected HEK293 cells were visualized in optical detection channels for CFP and FlAsH. As shown in Fig. 1 *A*, both CFP- and myc/C4-FlAsH-tagged ET_A and ET_B constructs were distinctly targeted to the plasma membrane of HEK293 cells.

Time course and reversibility of FlAsH incorporation

Stably transfected myc-ET_A-C4 or myc-ET_B-C4 in HEK293 cells were transfected with ET_A-CFP or ET_B-CFP, and fluorescence emission was measured every 4 min (details in Fig. 1 legend) in the CFP and FlAsH channels over a 100-min time course. Addition of 1 μM FlAsH resulted in a systematic drop in CFP fluorescence concomitant with a rise in FlAsH fluorescence, with both signals becoming saturated after ~70 min (Fig. 1 *B*). Incubation with 5 mM BAL, which displaces FlAsH from the tetracysteine binding site, quickly washed away the FlAsH acceptor and restored CFP fluorescence to near basal conditions. This step demonstrated a ready reversibility of the FRET signal. The recovery of CFP fluorescence after BAL addition to near basal levels showed that the effects of photobleaching on the system were minimal. Calculation of the FRET efficiency from this data was as follows: FRET efficiency = 1 − [1/FRET ratio], where FRET ratio = (CFP emission after FlAsH loading and BAL wash)/(CFP emission after FlAsH loading and before BAL wash).

ET receptor homo- and heterodimers in HEK293 cells by FRET

HEK293 cells stably expressing myc-ET_A-C4 or myc-ET_B-C4 were transiently transfected with ET_A-CFP or ET_B-CFP. In all cases, the transiently transfected construct was the FRET donor (CFP) and was expressed at a lower average level than the stably expressed construct (C4), which was the FRET acceptor (Table 1). Thus, with a saturating (or near-saturating) amount of FRET acceptor relative to donor, the system was optimized for reproducible FRET measurements. After equilibration with FlAsH, as shown in Fig. 1 *B*, FRET efficiencies of 15 ± 3%, 22 ± 2% and 27 ± 4% were observed for ET_A/ET_A, ET_B/ET_B, and ET_A/ET_B combinations, respectively. These values were reproducible among different regions of the plasma membrane and from cell to cell, plate to plate, and experiment to experiment. FRET effi-

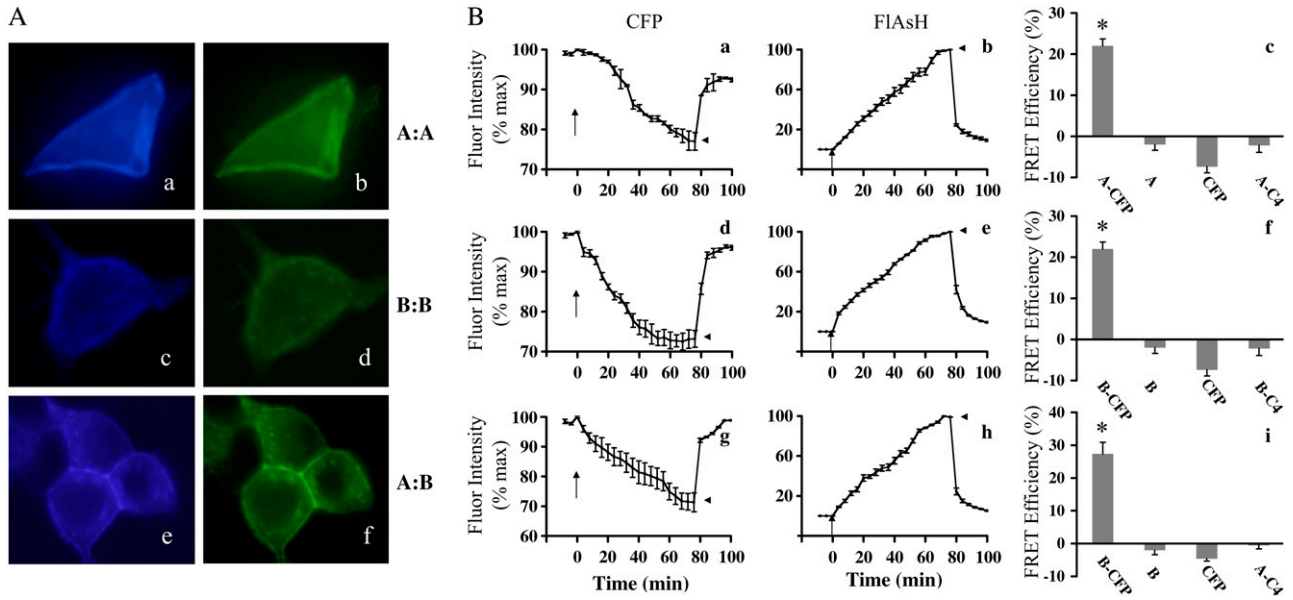

FIGURE 1 Localization and FRET interactions of donor (CFP)- and acceptor (FlAsH)-tagged ET receptors. Tetracysteine (C4)-fused constructs were made stable in HEK293 cells in all experiments. (*A*) ET_A-C4 transfected with ET_A-CFP (*a* and *b*) or ET_B-CFP (*e* and *f*) and ET_B-C4 transfected with ET_B-CFP (*c* and *d*) were visualized in the CFP channel (*left*) or the FlAsH channel (*right*). (*B*) Fluorescence intensity was measured once every 4 min (with 5×0.25 s = 1.25 s total exposure to excitation light per measurement) in both CFP and FlAsH channels in ET_A-C4 (*a*, *b*, *g*, and *h*) or ET_B-C4 (*d* and *e*) transfected with ET_A-CFP (*a* and *b*), or ET_B-CFP (*d*, *e*, *g*,and *h*); 1μM FlAsH added at the arrow; 5 mM BAL added at the arrowhead. Summary of FRET measurements of ET_A-C4 (*c* and *i*) or ET_B-C4 (*f*) transfected with ET_A-CFP (*c*) or ET_B-CFP (*f* and *i*); *A-CFP*, ET_A-CFP; *A*, ET_A; *A-C4*, ET_A-C4; *B-CFP*, ET_B-CFP; *B*, ET_B; *B-C4*, ET_B-C4; $*p < 0.05$ by one-way ANOVA with Tukey's post-test indicates significant difference from all others.

ciencies between 15% and 27% are indicative of robust endothelin-receptor homo- and heterodimerization. Incubation with FlAsH in the absence of myc-ET_A-C4 or myc-ET_B-C4, but in the presence of CFP-tagged ET_A or ET_B receptors did not produce a FRET signal. Transfection of nontagged ET_A or ET_B receptors, or CFP alone, to stably expressing myc-ET_A-C4 or myc-ET_B-C4 cells, or exposure of the stable cell lines to FlAsH alone, also gave no FRET signal (Fig. 1 *B*). The data indicate that the FRET signal is limited to CFP-tagged and FlAsH-bound C4-tagged receptors and therefore provides evidence for short-range protein-protein interactions between receptors.

Evidence for specificity of the FRET signal was obtained by a pharmacological analysis. Addition of ET-1 (10 nM) significantly reduced FRET efficiency in all dimers (Fig. 2). As a control, addition of 10 nM ET-1 to cells expressing CFP-tagged ET_A or CFP-tagged ET_B alone, or FlAsH-bound myc-ET_A-C4 or FlAsH-bound myc-ET_B-C4 alone, had no effect on CFP or FlAsH fluorescence. Thus, under conditions where no FRET was observed, ET-1 did not influence probe fluorescence. The effects of ET-1 on FRET efficiency were blocked by preincubation of ET_A homodimers with the ET_A selective antagonist BQ123 or ET_B homodimers with the ET_B selective antagonist BQ788 (Fig. 2). It is interesting that the FRET change observed for ET_A/ET_B heterodimers in response to ET-1 required the presence of both BQ123 and BQ788 for effective blockade (Fig. 2). Receptor subtype specificity was further demonstrated by incubation with 30 nM sarafotoxin s6c, an ET_B selective agonist. Sarafotoxin s6c reduced FRET efficiency by a similar magnitude to ET-1, but only in dimers containing ET_B (Fig. 2).

The FRET change observed with 10 nM ET-1 occurred within 30 s (the shortest time tested), as indicated by the dramatic and abrupt increase in CFP fluorescence after addition of ET-1 (Fig. 3). This rapid onset of the ET-1 response suggested that ET-1 reduces FRET efficiency predominantly by ligand binding and subsequent conformational change(s) rather than by processes occurring in the minute time domain, such as receptor internalization. Moreover, in the presence of 450 mM sucrose, which has previously been shown to prevent clathrin-mediated internalization (27), ET-1 caused changes in FRET efficiency similar in magnitude and direction to those observed in the absence of sucrose (15% to 7% for ET_A/ET_A, 22% to 15% for ET_B/ET_B, and 27% to 10% for ET_A/ET_B). In all dimers, addition of antagonists alone also tended to reduce FRET efficiency (as in Fig. 2), possibly representing an antagonist-induced dimer rearrangement. This is in agreement with a study showing that BQ123 can bind and induce a conformational change in ET_A (28); in our system, this phenomenon requires further investigation.

Receptor dimers by coimmunoprecipitation

In HEK293 cells stably expressing myc-tagged ET_A or ET_B receptors, immunoblots with an anti-c-myc monoclonal antibody detected a band at ~50 kD, corresponding to the myc-

TABLE 1 Radioligand binding characteristics of endothelin receptor dimers

Receptors	B_{max} (pmol/mg)	Percent of control*	C4/CFP†	Adjusted C4/CFP	Adjusted ET_A/ET_B
Homodimers					
myc-ET_A-C4 (control)	0.96 ± 0.06	100			
myc-ET_A-C4/ET_A-CFP	1.53 ± 0.05‡	159	1.69:1	0.85:1	
myc-ET_A-C4/ET_A-CFP, +BQ123	0.18 ± 0.08‡	12			
myc-ET_B-C4 (control)	7.07 ± 0.06	100			
myc-ET_B-C4/ET_B-CFP	12.06 ± 1.24‡	171	1.41:1	0.71:1	
myc-ET_B-C4/ET_B-CFP, +BQ788	0.24 ± 0.08‡	2			
Heterodimers					
myc-ET_A-C4/ET_B-CFP	1.40 ± 0.06‡	146	2.17:1	1.09:1	1.09:1
myc-ET_A-C4/ET_B-CFP, +BQ123/BQ788	0.05 ± 0.02§	4			
myc-ET_B-C4/ET_A-CFP	9.91 ± 0.77‡	140	2.50:1	1.25:1	0.80:1
myc-ET_B-C4/ET_A-CFP, +BQ123/BQ788	0.24 ± 0.10§	2			

Binding of [^{125}I]-ET-1 was performed as described in Materials and Methods. B_{max} is the density of specific ET-1 binding sites in pmol/mg protein measured in HEK293 cells. Data are the mean ± SE of at least three independent experiments, each performed in duplicate. BQ123 and BQ788, each applied at 1 μM, were used as receptor antagonists for ET_A and ET_B, respectively.

*HEK293 cells stably expressing myc-ET_A-C4 or myc-ET_B-C4 served as controls (100% specific binding). After transient transfection with ET_A-CFP or ET_B-CFP, the parameter ''percent of control'' represents a measure of specific ET-1 binding to stably plus transiently transfected receptors.

†The molar ratio of C4 to CFP tagged receptors calculated from ET-1 binding before (C4) and after (CFP) transient transfection. Adjusted C4/CFP ratio is calculated by assuming a uniform receptor density in stable cell lines and a 50% transient transfection efficiency. Adjusted ET_A:ET_B is the molar ratio of receptor subtypes estimated from the adjusted C4/CFP ratio.

‡$p < 0.05$ by Student's t-test between dimer and myc-ET_A-C4 or myc-ET_B-C4 control.

§$p < 0.05$ by Student's t-test between dimer and myc-ET_A-C4:ET_B-CFP or myc-ET_B-C4:ET_A-CFP.

ET_A-C4 or myc-ET_B-C4 receptor, that was absent in HEK293 cells alone. In addition, CFP-tagged ET_A or ET_B receptors expressed in HEK293 cells gave a band at ~75 kD on immunoblots with an anti-CFP monoclonal antibody. Therefore, the c-myc and CFP antibodies were deemed suitable for coimmunoprecipitation analysis. Next, stably expressed myc-ET_A-C4 or myc-ET_B-C4 receptors were transfected with ET_A-CFP or ET_B-CFP and subjected to detergent solubilization. ET_A and ET_B receptors were immunoprecipitated with the c-myc antibody and immunoblotted with the CFP antibody. A band at ~75 kD corresponding to the CFP-tagged ET_A or ET_B receptor was found in myc-ET_A-C4/ET_A-CFP and myc-ET_B-C4/ET_B-CFP, indicative of ET_A and ET_B homodimers (Fig. 4). In addition, a band at ~75 kD corresponding to ET_B-CFP was found in myc-ET_A-C4/ET_B-CFP, indicative of heterodimers. No band was seen in mock-transfected myc-ET_A-C4 and myc-ET_B-C4 stable cell lines. To rule out the possibility of receptor aggregation after solubilization, the following cell extracts were mixed after receptor solubilization but before immunoprecipitation: myc-ET_A-C4 plus ET_A-CFP (nonspecific ET_A homodimers), myc-ET_B-C4 plus ET_B-CFP (nonspecific ET_B homodimers), and myc-ET_A-C4 plus ET_B-CFP (nonspecific ET_A heterodimers). In agreement with a previous study (20), mixtures of cell extracts failed to result in coimmunoprecipitation of receptors.

It is important that preincubation of cells expressing ET receptors with the nonselective agonist ET-1 or the ET_B selective agonist sarafotoxin s6c had no effect on the ability to coimmunoprecipitate the tagged receptors (Fig. 4). These observations indicate that agonists do not promote dimer formation, nor do they dissociate dimers. Coimmunoprecip-

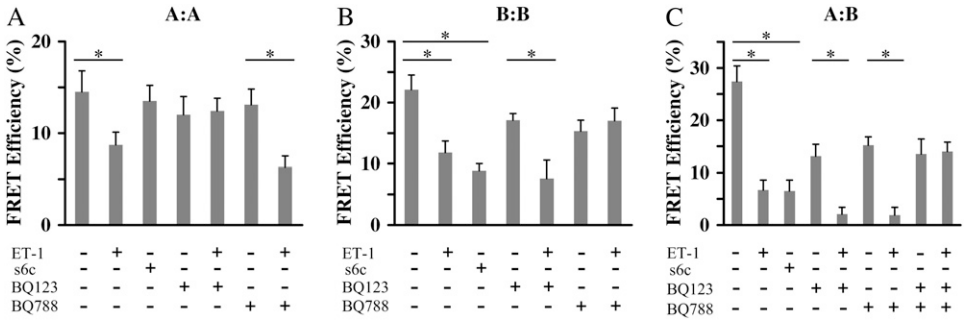

FIGURE 2 Ligand effects on FRET for homo- and heterodimers. HEK293 cells stably expressing ET_A-C4 (*A* and *C*) or ET_B-C4 (*B*) were transfected with ET_A-CFP (*A*) or ET_B-CFP (*B* and *C*). Cells were preincubated with 10 nM ET-1 or 30 nM s6c for 10 min at room temperature followed by FRET analysis. Cells treated with antagonists (1 μM BQ123 and BQ788) were preincubated for 10 min before ligand addition. Values are mean ± SE from at least 20 cells. *$p < 0.05$ by Student's t-test.

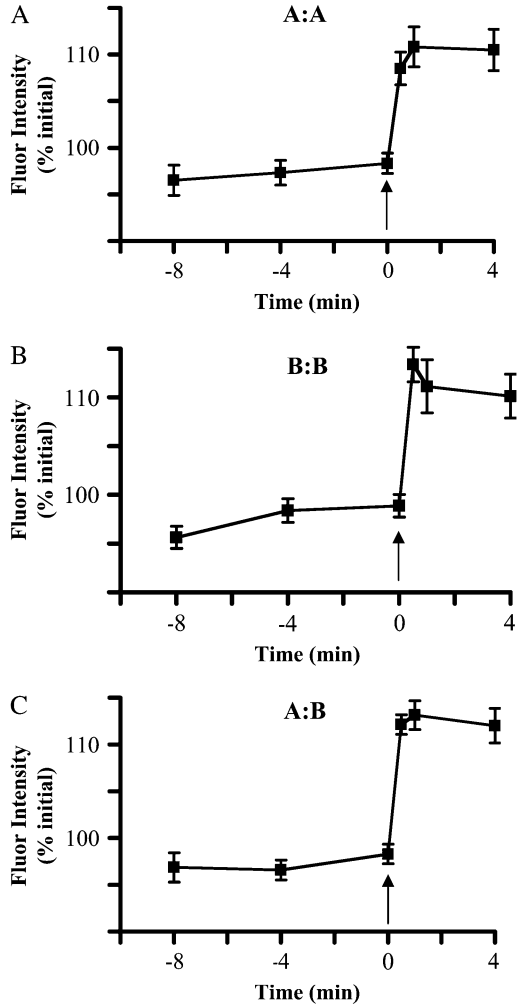

FIGURE 3 Time course of ET-1 effects on FRET. Stably expressed C4-tagged ET_A-C4 (*A* and *C*) or ET_B-C4 (*B*) were transfected with ET_A-CFP (*A*) or ET_B-CFP (*B* and *C*) in HEK293 cells. Cells were exposed to 10 nM ET-1 (*arrow*) and CFP fluorescence was measured at 30 s, 60 s, and 4 min. Values are mean ± SE from at least eight cells. Not shown here was a concomitant (but much smaller) decline in FlAsH fluorescence.

itation and FRET measurements revealed different but complementary aspects of ET dimerization.

Receptor density and pharmacology by [^{125}I]-ET-1 binding

A potential limitation of receptor overexpression in heterologous cell systems is the possibility that receptors achieve supraphysiological densities on the cell surface. Therefore, ET_A and ET_B receptor densities were measured using [^{125}I]-ET-1 binding in HEK293 cells (Table 1). The two stable HEK293 cell lines expressed 0.96 ± 0.06 pmol/mg protein for myc-ET_A-C4 cells and 7.07 ± 0.72 pmol/mg protein for myc-ET_B-C4. Upon subsequent transient transfection of ET_A-CFP or ET_B-CFP to generate homodimers, specific [^{125}I]-ET-1 binding increased by ~60% to 1.53 ± 0.05 pmol/mg and 12.06 ± 1.24 pmol/mg, respectively (Table 1). Specific binding was blocked by the appropriate antagonist, BQ123 for ET_A homodimers and BQ788 for ET_B homodimers (Table 1). For as yet unknown reasons, the ET_B constructs appeared to express more robustly than ET_A constructs for both transient transfection and stable expression. Nevertheless, these data are consistent with other estimates of ET receptor density in heterologous expression systems (9,10,20).

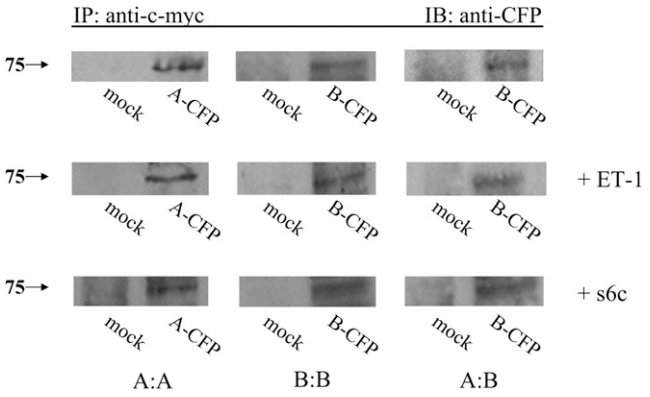

FIGURE 4 Coimmunoprecipitation of receptor constructs expressed in HEK293 cells. Stably transfected myc-ET_A-C4 (*left* and *right*) or myc-ET_B-C4 (*middle*) were transfected with ET_A-CFP (*left*) or ET_B-CFP (*middle* and *right*). Cells were subjected to no treatment, 10 nM ET-1, or 30 nM s6c for 10 min, solubilized in detergent, then immunoprecipitated with a monoclonal anti-myc antibody. Immunoprecipitated proteins were then immunoblotted using a monoclonal anti-CFP antibody.

HEK293 cells expressing ET_A/ET_B heterodimers were also evaluated by [^{125}I]-ET-1 binding. Transient transfection of ET_B-CFP in the myc-ET_A-C4 cell line increased [^{125}I]-ET-1 binding by ~50% (Table 1). The reciprocal order of expression involving transient transfection of ET_A-CFP in the myc-ET_B-C4 cell line also increased specific binding by ~40%, despite different total levels of receptor expression. This provided a useful comparison between HEK293 cells expressing significantly different overall densities of ET-1 binding sites, 1.40 ± 0.06 pmol/mg vs. 9.91 ± 0.77 pmol/mg, and somewhat different ET_A/ET_B ratios (1.09:1 vs. 0.80:1, Table 1). In both cases, complete blockade of [^{125}I]-ET-1 binding required the presence of both BQ123 and BQ788 (Table 1). In contrast, individual application of subtype-selective antagonists resulted in only partial blockade of [^{125}I]-ET-1 binding to heterodimers. For example, BQ123 reduced specific [^{125}I]-ET-1 binding from 1.40 ± 0.06 to 0.49 ± 0.09 (66% blockade) whereas BQ788 reduced specific [^{125}I]-ET-1 binding from 1.40 ± 0.06 to 0.92 ± 0.05 (34% blockade), consistent with the proportions of ET_A and ET_B expressed.

Functional consequences of receptor dimerization

To test the functional consequences of receptor homo- and heterodimerization, HEK293 cells expressing ET receptor

constructs were loaded with Ca^{2+}-sensitive dyes Fluo-4 or X-rhod-1. Cells were stimulated with agonists in the presence and absence of extracellular Ca^{2+}. A representative experiment is shown in Fig. 5 *A*. ET-1 stimulation of HEK293 cells expressing myc-ET_A-C4/ET_A-CFP and myc-ET_B-C4/ET_B-CFP resulted in a transient increase in Ca^{2+} indicator fluorescence within 1–2 min that returned toward basal levels after 2–4 min (Fig. 5 *B*). This transient response was similar to what was observed when the C4- or CFP-tagged receptors were expressed individually (29). Preincubation with the appropriate subtype-selective antagonist blocked this effect of ET-1 on intracellular Ca^{2+}. Removal of extracellular Ca^{2+} in the bathing solution had no effect on the response of ET_A homodimers, but ablated the response of ET_B homodimers to ET-1 (Fig. 5 *B*). This is consistent with ET_A receptors mobilizing Ca^{2+} through an IP_3-regulated intracellular store, whereas ET_B receptors rely more on Ca^{2+} influx from the extracellular solution (1–3,30). The ET_B selective agonist sarafotoxin s6c resulted in a similar transient increase in intracellular calcium, but only with ET_B homodimers. To address whether the transient nature of the homodimer response was due to dye bleaching or leakage, HEK293 cells were stimulated with the Ca^{2+} ionophore A23187. This resulted in a sustained increase of indicator fluorescence that lasted >30 min (data not shown), arguing against time-dependent changes in dye performance.

ET-1 stimulation of heterodimers did not show the transient Ca^{2+} increase seen with homodimers, but instead resulted in a Ca^{2+} signal that was sustained throughout the 10-min test period. Ca^{2+} elevation mediated by heterodimers was also not influenced by removal of extracellular Ca^{2+}, consistent with involvement of intracellular Ca^{2+} stores. The sustained Ca^{2+} elevation mediated by heterodimers could not be blocked by standard doses of the antagonists BQ123 or BQ788 alone, but was completely inhibited by application of BQ123 and BQ788 in combination at the same doses (Fig.

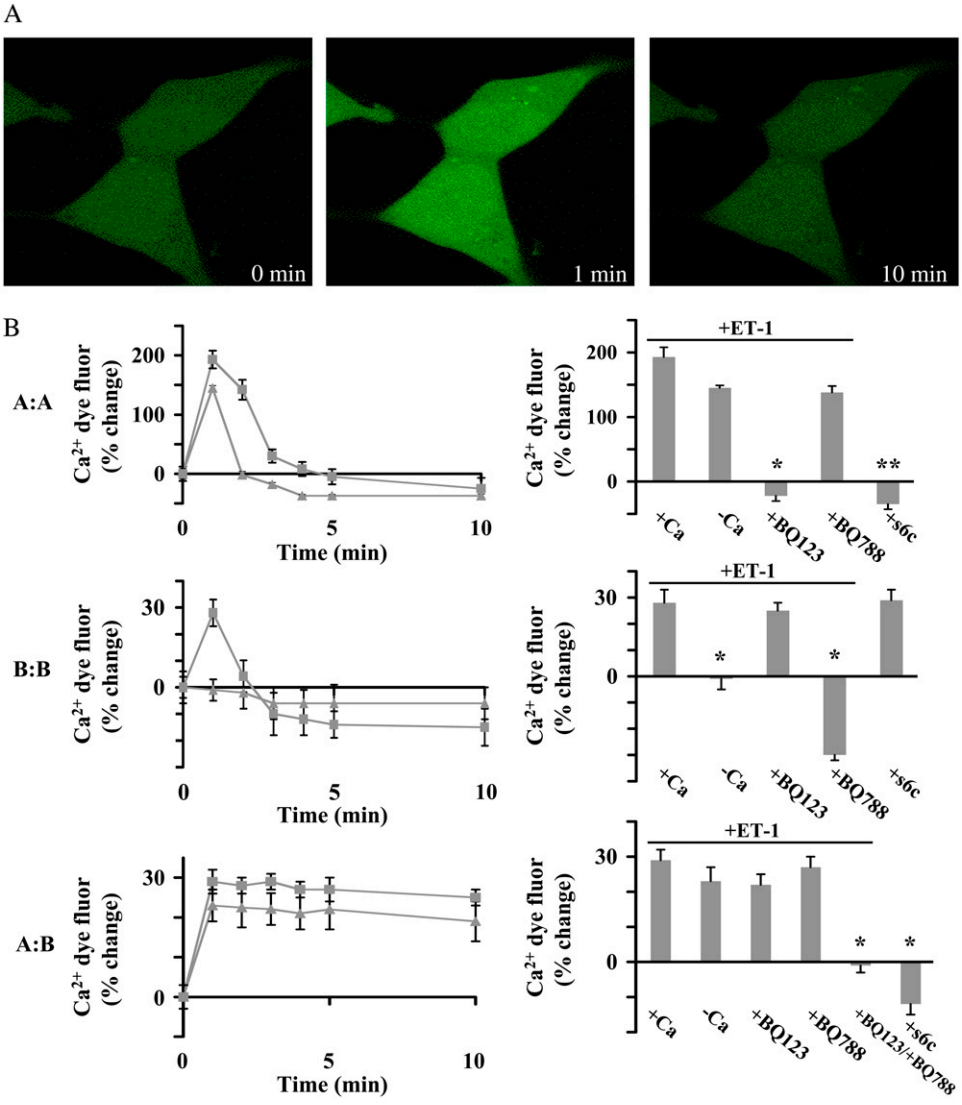

FIGURE 5 Intracellular Ca^{2+} mobilization mediated by receptor homo- and heterodimers. (*A*) Visualization of Fluo-4 loaded HEK293 cells stably expressing ET_A-C4 and transfected with ET_A-CFP stimulated by ET-1. (*B*) Stable ET_A-C4 transfected with ET_A-CFP (*upper*) or ET_B-CFP (*lower*), and stable ET_B-C4 transfected with ET_B-CFP (*middle*) were subjected to ligand treatment; extracellular solution with (*squares*) or without Ca^{2+} (*triangles*). Bar graphs summarize changes in indicator fluorescence after 1 min averaged over five to eight cells. Ca^{2+} signals mediated by heterodimers were sustained for >10 min even in the presence of BQ123 or BQ788 alone. $*p < 0.05$ by one-way ANOVA with Tukey's post-test indicates significant difference from all others, except those marked with two asterisks (**), and ** indicates significant difference among all others except those marked with one asterisk (*).

5 *B*). Heterodimers composed of myc-ET_A-C4/ET_B-CFP or myc-ET_B-C4/ET_A-CFP behaved indistinguishably. It is interesting that despite the fact that the ET_B selective antagonist sarafotoxin s6c could bind to ET_A/ET_B heterodimers, sarafotoxin s6c was unable to trigger Ca^{2+} mobilization for reasons that are not entirely clear.

Nevertheless, the data provide unique ligand binding and functional profiles for each of the ET receptor dimer species. ET_A/ET_A homodimers mediated a transient intracellular-store-dependent Ca^{2+} increase with traditional ET_A receptor pharmacology. ET_B/ET_B homodimers mediated a transient extracellular-pool-dependent Ca^{2+} increase with traditional ET_B receptor pharmacology. Finally, ET_A/ET_B heterodimers mediated a sustained intracellular-store-dependent Ca^{2+} increase with unique pharmacological properties. Specifically, heterodimers required combined ET_A and ET_B antagonism to inhibit ET-1 binding, subsequent conformational changes, and functional coupling.

DISCUSSION

The purpose of this study was to investigate homo- and heterodimerization of ET_A and ET_B receptors in HEK293 cells with an emphasis on elucidating the functional consequences of dimerization. The FRET efficiencies for ET receptor homo- and heterodimers reported here were in qualitative agreement with previous studies that examined ET receptor dimerization using CFP- and YFP-tagged receptors (20,21). Use of the FlAsH acceptor in place of YFP allowed for robust signals including FRET efficiencies up to 27% for ET_A/ET_B heterodimers with the microscope arrangement used. In previous studies with the CFP/YFP pair, receptor binding by ET-1 had no statistically significant effects on FRET efficiency, whereas in this study, use of the CFP/FlAsH pair revealed unambiguous ligand-dependent changes in FRET efficiency. Thus, to our knowledge, this is the first report of a FRET assay for monitoring ligand-induced conformational changes in ET-receptor dimers. FlAsH based FRET has been successfully employed to monitor conformational changes in adenosine receptor monomers (23), and a bioluminescence resonance energy transfer assay has been shown to detect isoproterenol binding to β_2-adrenergic receptor homodimers (31).

We proceeded to exploit this FRET signal to reveal the pharmacology of ET receptor dimers, and compared these properties with receptor pharmacology monitored by Ca^{2+} mobilization. The data provide strong evidence for functional and pharmacological properties that are unique to ET-receptor heterodimers. Specifically, we provided evidence that heterodimers undergo a conformational change that precedes a sustained (rather than transient) intracellular Ca^{2+} elevation in response to ET-1. This sustained intracellular Ca^{2+} elevation induced by ET-1 is in agreement with the results of a previous study (32). Moreover, ET-1 responses mediated byheterodimers required both an ET_A and an ET_B subtype-selective antagonist for effective inhibition of the conformational change, as well as the sustained Ca^{2+} response. Thus, if we can extrapolate these results to ET receptors in native tissues, subtype-selective antagonists may be relatively ineffective at blocking heterodimer function, compared to a mixture of antagonists or to antagonists with mixed specificity. Further investigation is required to reveal the precise properties of ET receptors in native tissues.

In contrast to heterodimers, ET-1 responses mediated by homodimers displayed a transient intracellular Ca^{2+} elevation, which was inhibited by inclusion of only the appropriate receptor subtype-selective antagonist: BQ123 for ET_A homodimers and BQ788 for ET_B homodimers. The FRET changes induced by ET-1 binding were also inhibited by the appropriate subtype-selective antagonist. Examination of the ET_B selective agonist sarafotoxin s6c showed the expected pharmacology, causing a $>$50% decrease in FRET that again preceded a transient elevation of intracellular Ca^{2+}. As expected, sarafotoxin s6c only affected ET_B homodimers, not ET_A homodimers. Thus, the pharmacological profile of homodimers monitored in this way was indistinguishable from isolated ET_A and ET_B binding sites and/or functional monomers. It has been previously demonstrated that fluorescent probes fused onto the C-terminus of ET_A and ET_B receptors or the c-myc epitope included on the N-terminus of the receptors have only minimal effects on function and ligand binding of ET receptors (9,20). Insertion on the C-terminus of other similar optical tags, including the C4 motif, have also been shown to have no effect on function in a variety of receptors (22–26,31). Recently, we have provided evidence that the fluorescent probes and the myc/C4 tags have minimal effects on receptor expression, trafficking, and overall receptor function (29).

In this study, we also sought to determine whether ET receptor dimerization was required for normal receptor trafficking to the cell surface of HEK293 cells. ET receptor FRET signals were not detected within intracellular compartments, but were only observed in the plasma membrane. This interpretation was further supported by examining an ET_A receptor point mutation (F376A) within a highly conserved rhodopsinlike GPCR export motif on the C-terminus (33,34). This mutation prevented surface membrane expression and effectively eliminated FRET throughout the cells for all dimers containing ET_A (data not shown). Thus, assuming that the F376A mutation had no effect on dimerization itself, the data suggest that receptors accumulate at the cell surface before dimerization proceeds. The results do not support a role for dimerization in ET receptor trafficking to the cell surface, at least in HEK293 cells. The extent of dimerization appeared to be largely independent of ligand, as preincubation with ET-1 or sarafotoxin s6c had no effect on the ability to coimmunoprecipitate tagged receptors. Therefore, overall, the data suggest that ET receptors form long-lived ''constitutive'' homo- and heterodimers that do not appear before surface membrane expression and whose overall de-

gree of association is not detectably influenced by ligand binding. These observations differ from other GPCRs such as the $GABA_B$ and β2-adrenergic receptors, which require dimerization for membrane trafficking (14,35) and differ from receptor tyrosine kinases, where ligands promote dimerization by effectively cross-linking monomeric receptors (36). Taken together, these considerations demonstrate the complexity and diversity of cell surface signaling and trafficking even within the GPCR superfamily.

What are the physiological implications of the unique functional characteristics of ET receptor heterodimers? The sustained Ca^{2+} signaling exhibited by ET heterodimers, even in the absence of extracellular Ca^{2+}, suggests novel signaling mechanisms involving intracellular Ca^{2+} stores. The sustained, rather than transient or oscillatory, nature of the Ca^{2+} increase raises the intriguing possibility that ET-1 is capable of initiating unique patterns of temporally and spatially controlled intracellular Ca^{2+} signals. For example, in rabbit and mouse ventricular myocytes, global systolic Ca^{2+} transients are known to initiate cyclic contractile activity, whereas ET-1 can initiate a completely distinct IP_3-mediated Ca^{2+} response (possibly sustained) that stimulates hypertrophic gene transcription (37). The ability of ET heterodimerization to expand receptor signaling diversity underscores the importance of understanding the pharmacological and functional consequences of these interactions.

The observation that each subtype-selective antagonist binds independently to heterodimers, but when used alone cannot block FRET changes or sustained Ca^{2+} mobilization, leads to several important insights. First, each ET-1 binding site in the heterodimer appears capable of independently activating conformational changes and coupling to sustained Ca^{2+} signaling. Second, the sustained Ca^{2+} response is likely mediated by heterodimers, and is not the result of a unique combination of intracellular signaling events initiated by activation of separate ET_A and ET_B receptors. If sustained Ca^{2+} responses were due to activation of separate cell surface ET_A and ET_B, then antagonists would be expected to convert the sustained Ca^{2+} response to a transient one. Third, the requirement for both ET_A- and ET_B-selective antagonists to inhibit function may be a hallmark of ET receptor heterodimer pharmacology. This is clearly not the whole story, however, and further investigation is required to determine the specific role(s) of each receptor ''subunit'' in heterodimer signaling. For example, in this study, the ET_B-selective agonist sarafotoxin induced a conformational change in heterodimers, but failed to produce a functional Ca^{2+} increase. Sarafotoxin s6c appears capable of binding to ET_B within the heterodimer, but is not capable of initiating the proper G-protein coupling necessary for signaling within the heterodimer. A more complete systematic analysis of agonist and antagonist binding to heterodimers is of interest and is currently underway.

It is well established that plasma ET-1 levels are elevated in patients with various chronic conditions including chronic heart failure (CHF), atherosclerosis, diabetes, and certain malignant tumors. For CHF, efforts to uncover the efficacy of ET receptor antagonists have yielded mixed results. Infusion or oral administration of the dual selective ET_A/ET_B antagonist Bosentan improved systemic and pulmonary hemodynamics (38–41), and infusion of the dual selective ET_A/ET_B antagonist Tezosentan reduced peripheral resistance and increased cardiac power in CHF patients (42). Conversely, results of the ENABLE (Endothelin Antagonist Bosentan for Lowering Cardiac Events in Heart Failure) study using low doses of orally administered Bosentan failed to demonstrate efficacy in severe heart failure patients (43). Effective therapeutic intervention for these diseases will almost certainly depend upon developing a clearer understanding of the role of ET receptor dimerization in these chronic conditions. An intriguing possibility is that the efficacy of current ET receptor antagonists could be improved by establishing which ones preferentially block monomers, homodimers, and/or heterodimers. In this regard, the optical assays described here should permit a systematic evaluation of which antagonists and agonists target which dimeric ET receptor species and at what doses.

This work was supported by grants RO1HL081386 and T32-HL07936 from the National Institutes of Health.

REFERENCES

1. Yanagisawa, M., H. Kurihara, S. Kimura, Y. Tomobe, M. Kobayashi, Y. Mitsui, Y. Yazaki, K. Goto, and T. Masaki. 1988. A novel potent vasoconstrictor peptide produced by vascular endothelial cells. *Nature.* 332:411–415.
2. Sakurai, T., M. Yanagisawa, Y. Takuwa, H. Miyazaki, S. Kimura, K. Goto, and T. Masaki. 1990. Cloning of a cDNA encoding a non-isopeptide-selective subtype of the endothelin receptor. *Nature.* 348:732–735.
3. Sakurai, T., M. Yanagisawa, and T. Masaki. 1992. Molecular characterization of endothelin receptors. *Trends Pharmacol. Sci.* 13:103–108.
4. Russell, F. D., and P. Molenaar. 2000. The human heart endothelin system: ET-1 synthesis, storage, release and effect. *Trends Pharmacol. Sci.* 9:353–359.
5. Clozel, M., G. A. Gray, V. Breu, B. M. Loffler, and R. Osterwalker. 1992. The endothelin ET_B receptor mediates both vasodilation and vasoconstriction in vivo. *Biochem. Biophys. Res. Commun.* 186:867–873.
6. Hirata, Y., T. Emori, S. Eguchi, K. Kanno, T. Imai, K. Ohta, and F. Marumo. 1993. Endothelin receptor subtype B mediates synthesis of nitric oxide by cultured bovine endothelial cells. *J. Clin. Invest.* 91: 1367–1373.
7. Haynes, W. G., and D. J. Webb. 1998. Endothelin as a regulator of cardiovascular function in health and disease. *J. Hypertens.* 16:1081–1098.
8. Abe, Y., K. Nakayama, A. Yamanaka, T. Sakurai, and K. Goto. 2000. Subtype-specific trafficking of endothelin receptors. *J. Biol. Chem.* 275:8664–8671.
9. Bremnes, T., J. D. Paasche, A. Mehlum, C. Sandberg, B. Bremnes, and H. Attramadal. 2000. Regulation and intracellular trafficking pathways of the endothelin receptors. *J. Biol. Chem.* 275:17596–17604.
10. Paasche, J. D., T. Attramadal, C. Sandberg, H. K. Johansen, and H. Attramadal. 2001. Mechanisms of endothelin receptor subtype-specific targeting to distinct intracellular trafficking pathways. *J. Biol. Chem.* 276:34041–34050.

11. Gomes, I., B. A. Jordan, A. Gupta, C. Rios, N. Trapaidze, and L. A. Devi. 2001. G protein-coupled receptor dimerization: implications in modulating receptor function. *J. Mol. Med.* 79:226–242.
12. Angers, S., A. Salahpour, and M. Bouvier. 2002. Dimerization: an emerging concept for G protein-coupled receptor ontogeny and function. *Annu. Rev. Pharmacol. Toxicol.* 42:409–435.
13. Milligan, G. 2004. G protein-coupled receptor dimerization: function and ligand pharmacology. *Mol. Pharmacol.* 66:1–7.
14. White, J. H., A. Wise, M. J. Main, A. Green, N. J. Fraser, G. H. Disney, A. A. Barnes, P. Emson, S. M. Foord, and F. H. Marshall. 1998. Heterodimerization is required for the formation of a functional $GABA_B$ receptor. *Nature.* 396:679–682.
15. Zhu, W. Z., K. Chakir, S. Zhang, D. Yang, C. Lavoie, M. Bouvier, T. E. Hebert, E. G. Lakatta, H. Cheng, and R. P. Xiao. 2005. Heterodimerization of β1- and β2-adrenergic receptor subtypes optimizes β-adrenergic modulation of cardiac contractility. *Circ. Res.* 97:244–251.
16. Barki-Harrington, L., L. M. Luttrell, and H. A. Rockman. 2003. Dual inhibition of β-adrenergic and angiotensin II receptors by a single antagonist: a functional role for receptor-receptor interaction in vivo. *Circulation.* 108:1611–1618.
17. Liang, Y., D. Fotiadis, S. Filipek, D. A. Saperstein, K. Palczewski, and A. Engel. 2003. Organization of the G protein-coupled receptors rhodopsin and opsin in native membranes. *J. Biol. Chem.* 278:21655–21662.
18. Hasselblatt, M., H. Kamrowski-Kruck, N. Jensen, L. Schilling, H. Kratzin, A. L. Siren, and H. Ehrenreich. 1998. ET_A and ET_B receptor antagonists synergistically increase extracellular endothelin-1 levels in primary rat astrocyte cultures. *Brain Res.* 785:253–261.
19. Harada, N., A. Himeno, K. Shigematsu, K. Sumikawa, and M. Niwa. 2002. Endothelin-1 binding to endothelin receptors in the rat anterior pituitary gland: possible formation of an ET_A-ET_B receptor heterodimer. *Cell. Mol. Neurobiol.* 22:207–226.
20. Gregan, B., J. Jurgensen, G. Papsdorf, J. Furkert, M. Schaefer, M. Beyermann, W. Rosenthal, and A. Oksche. 2004. Ligand-dependent differences in the internalization of endothelin A and endothelin B receptor heterodimers. *J. Biol. Chem.* 279:27679–27687.
21. Gregan, B., M. Schaefer, W. Rosenthal, and A. Oksche. 2004. Fluorescence resonance energy transfer analysis reveals the existence of endothelin-A and endothelin-B receptor homodimers. *J. Cardiovasc. Pharmacol.* 44:S30–S33.
22. Adams, S. R., R. E. Campbell, L. A. Gross, B. R. Martin, G. K. Walkup, Y. Yao, J. Llopis, and R. Y. Tsien. 2001. New biarsenical ligands and tetracysteine motifs for protein labeling in vitro and in vivo: synthesis and biological applications. *J. Am. Chem. Soc.* 124:6063–6076.
23. Hoffmann, C., G. Gaietta, M. Bunemann, S. R. Adams, S. Oberdorff-Maass, B. Behr, J. P. Vilardaga, R. Y. Tsien, M. H. Ellisman, and M. J. Lohse. 2005. A FlAsH-based FRET approach to determine G protein-coupled receptor activation in living cells. *Nat. Methods.* 2:171–176.
24. Griffin, B. A., S. R. Adams, and R. Y. Tsien. 1998. Specific covalent labeling of recombinant protein molecules inside living cells. *Science.* 281:269–272.
25. Nakanishi, T., T. Takarada, S. Yunoki, Y. Kikuchi, and M. Maeda. 2006. FRET-based monitoring of conformational change of the β2 adrenergic receptor in living cells. *Biochem. Biophys. Res. Commun.* 343:1191–1196.
26. Andresen, M., R. Schmitz-Salue, and S. Jakobs. 2004. Short tetracysteine tags to β-tubulin demonstrate the significance of small labels for live cell imaging. *Mol. Biol. Cell.* 15:5616–5622.
27. Oksche, A., G. Boese, A. Horstmeyer, J. Furkert, M. Beyermann, M. Bienert, and W. Rosenthal. 2000. Late endosomal/lysosomal targeting and lack of recycling of the ligand-occupied endothelin B receptor. *Mol. Pharmacol.* 57:1104–1113.
28. Bhowmick, N., P. Narayan, and D. Puett. 1998. The endothelin subtype A receptor undergoes agonist- and antagonist-mediated internalization in the absence of signaling. *Endocrinology.* 139:3185–3192.
29. Evans, N. J., and J. W. Walker. 2008. Sustained Ca^{2+} signaling and delayed internalization associated with endothelin receptor heterodimers linked through a PDZ finger. *Can. J. Physiol. Pharm.* In press.
30. Maxwell, M. J., R. G. Goldie, and P. J. Henry. 1998. Ca^{2+} signaling by endothelin receptors in rat and human cultured airway smooth muscle cells. *Br. J. Pharmacol.* 125:1768–1778.
31. Angers, S., A. Salahpour, E. Joly, S. Hilairet, D. Chelsky, M. Dennis, and M. Bouvier. 2000. Detection of β2-adrenergic receptor dimerization in living cells using bioluminescence resonance energy transfer (BRET). *Proc. Natl. Acad. Sci. USA.* 97:3684–3689.
32. Dai, X., and J. J. Galligan. 2006. Differential trafficking and desensitization of human ET_A and ET_B receptors expressed in HEK293 cells. *Exp. Biol. Med.* 231:746–751.
33. Probst, W. C., L. A. Snyder, D. I. Schuster, J. Brosius, and S. C. Sealfon. 1992. Sequence alignment of the G-protein coupled receptor superfamily. *DNA Cell Biol.* 11:1–20.
34. Bermak, J. C., M. Li, C. Bullock, and Q. Y. Zhou. 2001. Regulation of transport of the dopamine D1 receptor by a new membrane-associated ER protein. *Nat. Cell Biol.* 3:492–498.
35. Salahpour, A., S. Angers, J. F. Mercier, M. Lagace, S. Marullo, and M. Bouvier. 2004. Homodimerization of the β2-adrenergic receptor as a prerequisite for cell surface targeting. *J. Biol. Chem.* 279:33390–33397.
36. Ottensmeyer, F. P., D. R. Beniac, R. Z. Luo, and C. C. Yip. 2000. Mechanism of transmembrane signaling: insulin binding and the insulin receptor. *Biochemistry.* 39:12103–12112.
37. Wu, X., T. Zhang, J. Bossuyt, X. Li, T. A. McKinsey, J. R. Dedman, E. N. Olson, J. Chen, J. H. Brown, and D. M. Bers. 2006. Local $InsP_3$-dependent perinuclear Ca^{2+} signaling in cardiac myocyte excitation-transcription coupling. *J. Clin. Invest.* 116:675–682.
38. Sitbon, O., M. Beghetti, J. Petit, L. Iserin, M. Humbert, V. Gressin, and G. Simonneau. 2006. Bosentan for the treatment of pulmonary arterial hypertension associated with congenital heart defects. *Eur. J. Clin. Invest.* 36:25–31.
39. Spieker, L. E., G. Noll, F. T. Ruschitzka, and T. F. Luscher. 2001. Endothelin receptor antagonists in congestive heart failure: a new therapeutic principle for the future? *J. Am. Coll. Cardiol.* 37:1493–1505.
40. Ertl, G., and J. Bauersachs. 2004. Endothelin receptor antagonists in heart failure. *Drugs.* 64:1029–1040.
41. Sutsch, G., W. Kiowski, X. W. Yan, P. Hunziker, S. Christen, W. Strobel, J. H. Kim, P. Rickenbacher, and O. Bertel. 1998. Short-term oral endothelin-receptor antagonist therapy in conventionally treated patients with symptomatic severe chronic heart failure. *Circulation.* 98:2262–2268.
42. Cotter, G., W. Kiowski, E. Kaluski, I. Kobrin, O. Milovanov, A. Marmor, J. Jafari, L. Reisin, R. Krakover, Z. Vered, and A. Caspi. 2001. Tezosentan (an intravenous endothelin receptor A/B antagonist) reduces peripheral resistance and increases cardiac power therefore preventing a steep decrease in blood pressure in patients with congestive heart failure. *Eur. J. Heart Fail.* 3:457–461.
43. Kalra, P. R., J. C. Moon, and A. J. Coats. 2002. Do results of the ENABLE (Endothelin Antagonist Bosentan for Lowering Cardiac Events in Heart Failure) study spell the end for non-selective endothelin antagonism in heart failure? *Int. J. Cardiol.* 85:195–197.